NMR Solution Structure of the Isolated N-Terminal Fragment of Protein-G B_1 Domain. Evidence of Trifluoroethanol Induced Native-like β-Hairpin Formation†

Francisco J. Blanco,‡ M. Angeles Jiménez, Antonio Pineda,§ Manuel Rico, Jorge Santoro, and José L. Nieto*

Instituto de Estructura de la Materia, Consejo Superior de Investigaciones Científicas, Serrano 119, 28006 Madrid, Spain

Received December 17, 1993; Revised Manuscript Received March 2, 1994®

ABSTRACT: The solution structure of the isolated N-terminal fragment of streptococcal protein-G B_1 domain has been investigated in H_2O and TFE/H_2O solution by CD and NMR to gain insight into the possible role that native β-hairpin secondary structure elements may have in early protein folding steps. The fragment also has been studied under denaturing conditions (6 M urea), and the resulting NMR chemical shifts were used as a reference for the disordered state. On the basis of CD and NMR data, it is concluded that in aqueous solution the fragment is basically flexible, with two local low populated chain bends involving residues 8–9 and 14–15, respectively, in close agreement with secondary structure predictions, a structure that is different from the final folded state of that segment of the protein. The changes in the CD spectrum, the presence of several medium-range NOEs plus two long-range NOEs, and the sign of the Hα conformational shifts reveal that the addition of TFE facilitates the formation of a set of transient β-hairpins involving essentially the same residues that form the native β-hairpin found in the final three-dimensional structure of the B_1 domain. The stabilization of native-like structures by TFE is known to occur for helices, but, to our knowledge, this is the first time the stabilization of a native-like β-hairpin structure by TFE is reported. Since long-range tertiary interactions are absent in the isolated fragment, our results support the idea that, in addition to helices, β-hairpins may play an active role in directing the protein folding process.

Native-like helix formation in aqueous solution has been demonstrated to occur in many isolated protein fragments that span helical regions of the corresponding protein structures (Bierzynsky et al., 1982; Rico et al., 1983; Jiménez et al., 1987, 1988; Dyson et al., 1992). This fact strongly supports the idea that helices act as nucleation centers in early stages of the protein folding process. From these results, it seems reasonable to postulate that other types of secondary structures, in particular β-turns or β-hairpins that are stabilized by short-range interactions, may also play a role in early folding. Although β-turns have been detected in several protein fragments in aqueous solution (Dyson et al., 1985, 1991; Reed et al., 1988; Chandrasekhar et al., 1993), only in very few cases (Blanco et at., 1991; Sönnischen et al., 1992; Shin et al., 1993) were the turns found in solution those seen in the native structure of the protein. In other cases, the native structure corresponding to the chain segment investigated was not a β-turn (Dyson et al., 1985) or the protein structure was not known (Reed et al., 1988; Chandrasekhar et al., 1991; Williamson et al., 1986; Bansai & Gierasch, 1991). No evidence is available so far of the existence of native β-hairpins in short protein fragments (Dyson et al., 1991). Still, short β-hairpins may have stability enough to exist as isolated entities in aqueous solution as reported recently for a designed peptide (Blanco et al., 1993).

In our search for potential β-hairpin nucleation centers in proteins, we have centered our attention on the B_1 domain of the streptococcal protein-G. The NMR[1] solution structures of this particular domain (Gronenborn et al., 1991) and other homologous domains (Lian et al., 1991; Orban et al., 1992) have been recently determined. The B_1 domain of protein-G, despite its small size and absence of disulfide bridges, is extremely resistant to denaturation induced either by heating or urea addition (Gronenborn et al., 1991; Alexander et al., 1992). The possibility that the unusual stability of the B_1 domain arises from the secondary structure preferences of its elements, in particular the two very well defined β-hairpins found in the protein structure (Figure 1), is therefore being examined by CD and NMR conformational studies of the peptide fragment that spans one of the β-hairpins, the N-terminal one that involves residues 2–19. On the basis of the NOE pattern, NOE intensities, and proton chemical shifts, it is concluded that the 2–19 fragment of the B_1 domain is not totally random in aqueous solution, signs of two local chain bends being detected at residues 8–9 and 14–15, chain regions close, although not coincident, to the native β-turn region (Figure 1).

Since there is increasing experimental evidence that TFE may induce structure stabilization in isolated protein fragments (Nelson & Kallenbach, 1989; Peña et al., 1989; Segawa et al., 1991; Jiménez et al., 1992; Dyson et al., 1992), we have also examined the conformation of the N-terminal fragment of the B_1 domain in aqueous trifluoroethanol. It will be shown that the addition of TFE results in the population of a folded conformation of the 2–19 fragment, different from the one detected in water. According to CD, NOE, and chemical shift data, the folded conformation consists of a set of transient β-hairpins structures, the β-turn of which spans residues 8–11, nearly the same residues that are involved in the native β-turn

† This work was supported by Grant PB90-1020 from the Spanish Ministry of Education.

* Address correspondence to this author (fax: 34-1-5642431).

‡ Present address: European Molecular Biology Laboratory, Heidelberg, Germany.

§ Centro de Investigaciones Biológicas, Consejo Superior de Investigaciones Científicas, Madrid, Spain.

® Abstract published in *Advance ACS Abstracts,* April 15, 1994.

[1] Abbreviations: CD, circular dichroism; NMR, nuclear magnetic resonance; TFE, trifluoroethanol; HPLC, high-pressure liquid chromatography; NOESY, two-dimensional nuclear Overhauser effect spectroscopy; ROESY, rotating frame exchange spectroscopy; COSY, correlation spectroscopy; TOCSY, total correlation spectroscopy; NOE, nuclear Overhauser effect; RMSD, root mean square deviation.

0006-2960/94/0433-6004$04.50/0

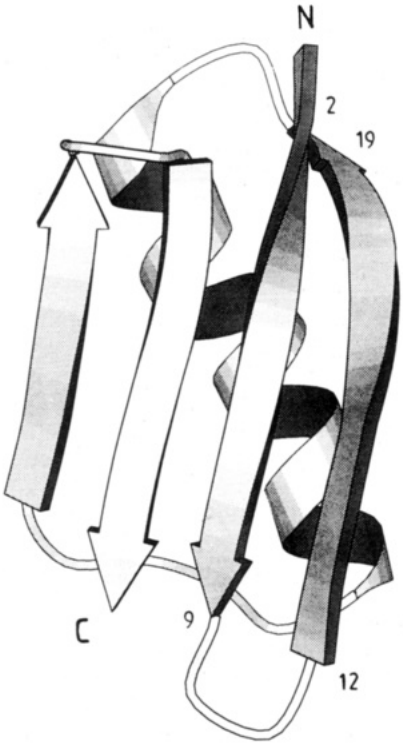

FIGURE 1: Ribbon three-dimensional structure of the B_1 domain of streptococcal protein-G, obtained with the program Molscript (Kraulis, 1991) (Protein Data Bank structure number 2GB1).

(residues 9–12) found in the three-dimensional structure of the protein. Although the origin and mechanism of stabilization remains unknown (Nelson & Kallenbach, 1986; Bruch et al., 1989; Sönnichen et al., 1992), this study and others (Macquaire et al., 1992, 1993; Buck et al., 1993; Rizo et al., 1993; Zhong & Johnson, 1992) support the notion that membrane-mimicking environments may favor the formation of native-like structures in polypeptide chains.

EXPERIMENTAL PROCEDURES

Materials. The peptide was chemically synthesized by Neosystem Laboratoire (Strasbourg, France). 2,2,2-Trifluoroethanol-d_3 was purchased from Cambridge Isotope Laboratories (Cambridge, MA). Urea was from Fluka Chemie, AG (Buchs, Switzerland).

CD Spectra. Circular dichroism spectra were recorded at 5 °C on a Jasco J-720 spectropolarimeter from Japan Spectroscopic Co. (Tokyo, Japan) interfaced to a Jasco data system. A water bath was used to obtain the desired temperature in the cell. Ellipticity is reported as mean residue molar ellipticity. Path lengths of 1 mm and 0.1 mm were used. Peptide concentrations were measured by ultraviolet absorbance (Gill & von Hippel, 1989). Secondary structure content was evaluated using three different methods that consider four structure types, helix, turn, sheet, and coil, specifically those proposed by Bolotina et al. (1980) and Chang et al. (1978) [incorporated into the Antheprot software package developed by Deleage and Geourjon (1993) and Yang et al. (1986) (standard in the Jasco dichrograph software)].

Proton NMR Spectra. The free peptide was dissolved in 0.4 mL of H_2O/D_2O in a 9:1 ratio by volume or in 3:7 TFE-d_3/H_2O, and the pH was then adjusted to 3.0 using a glass microelectrode. The peptide concentration was 5 mM. For experiments in denaturing conditions the appropriate amount of urea was added to the NMR sample, and the pH was readjusted. The temperature of the NMR probe was calibrated using a methanol sample. The NMR chemical shifts were measured with reference to internal sodium 3-trimethylsilyl [2,2,3,3-^{2}H]propionate (TSP). The ^{1}H NMR spectra were acquired on a Bruker AMX-600 pulse spectrometer. One-dimensional spectra were acquired using 32K data points, which were zero-filled to 64K data points before performing the Fourier transformation. Phase-sensitive two-dimensional COSY, TOCSY, NOESY, and ROESY spectra were recorded by standard techniques (Kessler et al., 1988) using presaturation of the water signal and the time-proportional phase incrementation mode. Mixing times were 150 ms for the NOESY and ROESY spectra. TOCSY spectra were recorded using a 60-ms MLEV 17 spin-lock sequence (Bax & Davis, 1985). Typically, 700 experiments were collected in t_1, each containing 2K data points. Additional TOCSY and NOESY spectra were recorded at the slightly more acidic pH 2.5 to solve assignment ambiguities. Data were processed using the standard UXNMR Bruker programs. The 2D data matrix was multiplied by a square-sine-bell window function, the corresponding phase shift being adjusted between $\pi/2$ and $\pi/3$ radians. Data matrix was zero filled and Fourier transformed into a 4K × 2K complex matrix. Baseline correction was applied in both dimensions. The intensity of all nonoverlapping NOE cross peaks was evaluated by volume integration. In case of partially overlapping cross peaks, the overall intensity was distributed in proportion to the relative height of the 1D peaks from the appropriate row of the 2D matrix transformed with digital resolution enhancement in both dimensions.

Size-Exclusion Chromatography. Possible aggregation of the 2–19 peptide was monitored at 5 °C in two solvent conditions (H_2O and TFE/H_2O) using a HR 10/10 Sephadex G-25 Superfine gel-filtration column (10 × 1 cm) mounted in a "Smart" HPLC chromatography system from Pharmacia. The conditions were 10 mM NaOAc, pH 3.0, 0.4 mL/min flow rate for the aqueous chromatography and 10 mM NaOAc, 100 mM NaCl, pH 3.0, 0.1 mL/min for the runs in 30% TFE/H_2O (Fan et al., 1993). The volume of the injections was 20 μL in both cases, taken from the corresponding NMR samples. Short peptides with molecular masses of 1205, 2167, and 3807 daltons were used as standards for calibration.

Secondary Structure Predictions. The method of Chou and Fasman (1977) was used to compute the turn probabilities all along the peptide chain of the 2–19 fragment. Recent methods proposed to identify conformational preferences of protein backbone segments [programs Prelude (Rooman et al., 1991) and Fugue (Rooman et al., 1992)] were also used.

Structure Calculations. Integrated NOE intensities were used to obtain upper limit distance constraints. A distance of 2.3 Å (somewhat larger that the value adopted in standard β-strands) was assigned to the most intense of the sequential αN NOEs and used for distance calibration. An averaging model (Braun et al., 1983) was used to derive all other distance constraints from observed NOE intensities. To these constraints, pseudoatom corrections were added where necessary. The final set of constraints comprised 6 intraresidual, 22 sequential, 20 medium-range and 1 long-range NOEs. Structures were calculated on a Silicon Graphics Indigo computer using the program DIANA (Güntert et al., 1991) and the REDAC strategy (Güntert & Wüthrich, 1991). Starting from 200 randomized conformations, the 20 best conformers were selected for the final runs. All these conformers satisfied the constraints with no violation greater than 0.1 Å. The high values of the pairwise RMSD, 2.9 ± 1.3 Å, showed that more than one structure could accounted

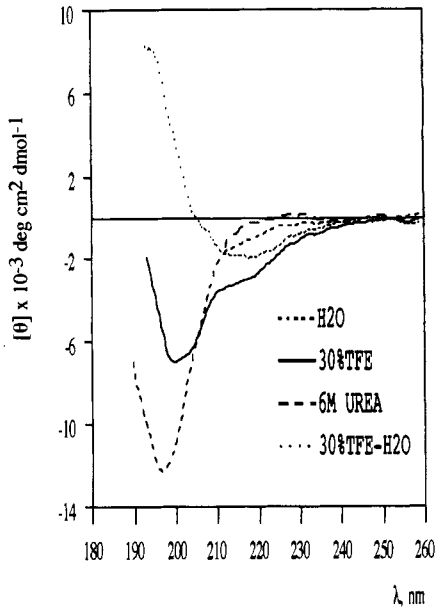

FIGURE 2: Circular dichroism spectra of the 2–19 fragment of protein-G B_1 domain recorded at 5 °C, pH 3.0, in various solvent conditions.

for the observed NOEs. A closer inspection of the computed structures allowed to classify them into four families with RMSDs values lower than 2 Å.

RESULTS

CD Spectra. The CD spectra of protein-G B_1 domain 2–19 fragment in different experimental conditions (H_2O, 30% TFE/H_2O, and 6 M urea) are shown in Figure 2. The difference CD spectrum between 30% TFE/H_2O and H_2O solution is also shown.

NMR Spectra. Proton NMR spectra were assigned using the standard sequential assignment procedure (Wüthrich et al., 1984). Table 1 shows the chemical shifts of the proton resonances of protein-G 2–19 fragment in the three solvent conditions studied, H_2O, 30% TFE/H_2O, and 6 M urea (pH 3.0, 5 °C). Figures 3 and 4 show selected regions of the NOESY spectra of the fragment in H_2O and TFE/H_2O solution, respectively. A ROESY spectrum of the fragment in TFE/H_2O, recorded in the same conditions, showed the long-range NOEs given in Figure 4 (Supplementary Material), thus indicating they are not spin diffusion artifacts. A NOESY spectrum run in TFE/H_2O using a very short mixing time (80 ms) showed NOE cross peaks of smaller intensity, as expected, but still most of the diagnostic NOEs, in particular the two aforementioned long-range NOEs and the NN(i,i+2) and NN(i,i+3) NOEs shown in Figure 4, also appear, thus confirming that spin diffusion is not important (Supplementary Material). A summary of observed NOEs in H_2O and TFE/H_2O including relative intensities of the short-range NOEs is given in Figure 5. The possible presence of aggregation was checked by diluting the H_2O and TFE/H_2O NMR samples by a factor of 50 (5 to 0.1 mM), with no appreciable changes in either line widths or chemical shifts being observed (data not shown). In TFE/H_2O solution a long-range NOE was present connecting the 2,6 protons of the side chain of Tyr 3 to the Hα protons of either Glu 15 or Thr 18 (Figure 4). A slight change of pH from 3.0 to 2.5 was sufficient to fully resolve the ambiguity and identify Thr 18 as the partner of Tyr 3 (Supplementary Material). A second long-range NOE connecting the same 2,6 side chain protons of Tyr 3 to the methyl group of Thr 17 or Thr 18 was also detected (Figure 4), but the ambiguity could not be definitively resolved and it was not included in the structure calculation. The amide shift temperature dependence was measured using δ values of a series of TOCSY spectra run at four temperatures within the range 4–36 °C. The corresponding $\Delta\delta/\Delta T$ values are shown in Table 1.

It is possible to detect differences in the conformational preferences of the peptide, in a qualitative way, by examining how the intensities of the NOEs are distributed all along the peptide chain, and their variations after a modification of the experimental conditions. To this end, the intensities of the short-range NOEs have been evaluated by volume integration of the corresponding cross peaks and normalized with reference to the largest sequential NOE cross peak, the αN NOE connecting residues 6–7 under all conditions examined. This procedure gives more structural information than the routine classification of NOE intensities into three size categories, based on visual inspection of contour levels. The use of a sequential αN NOE as the intensity reference was adopted rather than the *ortho–meta* Tyr side chain proton distance because backbone protons should have similar correlation times. Figure 5 shows the relative intensities of all measurable short-range NOEs plotted against the peptide sequence under two solvent conditions.

Proton Chemical Shifts. It is well established that chemical shift deviations from "random coil" reference values (Bundi & Wüthrich, 1979) (conformational shifts) closely correlate with the type of secondary structure in proteins (Jiménez et al., 1987; Williamson, 1990; Wishart et al., 1991) and peptides (Bruix et al., 1990; Andersen et al., 1992; Jiménez et al., 1992; Rizo et al., 1993). In particular Hα conformational shifts have been proposed to detect (Bruix et al., 1990), characterize (Blanco et al., 1992b), and also quantitate (Bruix et al., 1990; Blanco et al., 1992a; Rizo et al., 1993; Jiménez et al., 1994) low populated peptide helical structures in solution. Chemical shifts have an important advantage over NOEs in cases where conformational equilibria exist, the observed δ values are linear population-weighted averages over the different exchanging conformers. Uncertainties about local variation in effective correlation times do not affect the interpretation of averaged δ values in structural terms.

It should be noted that if chemical shift values of reference random tetrapeptides (Bundi & Wüthrich, 1979) are used to compute the conformational shifts in peptides, anomalous values may be obtained due to the influence on δ values of the amino acid sequence, which is different in the peptide under study and the reference peptides. The use, as a reference for the coil state, of the Hα δ values of the same peptide sequence investigated under denaturing conditions, 6 M urea, may thus yield more reliable conformational shifts, particularly if they result from small populations of folded structures. If evaluated in this way, chemical shifts are a very sensitive and powerful probe for detecting a minor folded structure of a peptide (Jiménez et al., 1994). The shifts must, of course, be larger than those expected for urea addition to a "random coil" peptide, values that have been measured in a series of random tetrapeptides (Jiménez et al., 1986, 1994) and found to be very small. The Hα conformational shifts of the 2–19 fragment, evaluated as differences between δ values in H_2O and urea, are represented against the peptide sequence in Figure 5a. In a similar way, the Hα δ differences between H_2O and TFE/H_2O should correlate with the conformational change effected by the addition of TFE. The effect of TFE addition on δ values of random peptides has been experi-

Table 1: Chemical Shifts (ppm from TSP) and NH Temperature Dependence of the 2–19 Fragment (pH 3.0, 5 °C)

	NH	αCH	βCH	γCH	δCH	other	$-\Delta\delta_{NH}/\Delta T$ (ppb/K)
				(A) Solvent: Water			
Thr 2		3.84	4.10	1.29			
Tyr 3	8.90	4.61	2.98, 3.00			2,6 H 7.12; 3,5 H 6.82	8.2
Lys 4	8.26	4.20	1.62, 1.68	1.28, 1.32	1.62	εH 2.94; NH_3^+ 7.59	5.0
Leu 5	8.30	4.26	1.52, 1.56	1.56	0.90, 0.95		7.8
Ile 6	8.42	4.15	1.82	1.16, 1.47	0.83	γCH_3 0.86	8.7
Leu 7	8.61	4.40	1.55, 1.63	1.63	0.86, 0.92		8.7
Asn 8	8.68	4.67	2.80, 2.87			NH_2 7.03, 7.75	8.7
Gly 9	8.56	3.90, 3.96					6.7
Lys 10	8.31	4.41	1.78, 1.86	1.40, 1.46	1.68	εH 2.99; NH_3^+ 7.61	6.7
Thr 11	8.32	4.33	4.18	1.20			7.8
Leu 12	8.47	4.37	1.59, 1.63	1.63	0.87, 0.92		7.8
Lys 13	8.49	4.27	1.78, 1.83	1.43	1.68	εH 2.98; NH_3^+ 7.61	7.8
Gly 14	8.58	3.96, 3.96					7.8
Glu 15	8.33	4.48	2.02, 2.15	2.48			5.5
Thr 16	8.48	4.47	4.27	1.22			7.8
Thr 17	8.42	4.47	4.27	1.21			7.8
Thr 18	8.37	4.37	4.22	1.22			7.3
Glu 19	8.48	4.36	1.97, 2.19	2.46			9.1
				(B) Solvent: 30% TFE/H_2O by Volume			
Thr 2		3.92	4.21	1.35			
Tyr 3	8.79	4.75	3.01, 3.06			2,6 H 7.16; 3,5 H 6.86	7.6
Lys 4	8.28	4.35	1.70, 1.78	1.36, 1.40	1.70	εH 3.00	7.3
Leu 5	8.10	4.45	1.62	1.62	0.93, 0.99		7.3
Ile 6	8.20	4.26	1.89	1.19, 1.52	0.89	γCH_3 0.90	8.6
Leu 7	8.33	4.48	~1.52	~1.52	0.93		8.6
Asn 8	8.49	4.72	2.84, 2.94				8.0
Gly 9	8.58	3.88, 4.01					6.6
Lys 10	8.28	4.43	1.88, 1.96	1.47, 1.53	1.74	εH 3.04	6.3
Thr 11	8.14	4.40	4.30	1.27			5.1
Leu 12	8.31	4.43	~1.68	~1.68	0.91, 0.97		7.9
Lys 13	8.33	4.36	1.84, 1.92	1.47, 1.53	1.74	εH 3.04	8.1
Gly 14	8.40	3.98, 4.08					5.9
Glu 15	8.31	4.58	2.08, 2.22	2.52			5.7
Thr 16	8.26	4.56	4.33	1.26			5.7
Thr 17	8.23	4.46	4.30	1.28			5.7
Thr 18	8.33	4.58	4.34	1.28			6.0
Glu 19	8.33	4.43	2.04, 2.24	2.51			7.2
				(C) Solvent: Water + 6 M Urea			
Thr 2		3.85	4.13	1.30			
Tyr 3	8.93	4.64	2.98, 3.00			2,6 H 7.11; 3,5 H 6.83	7.0
Lys 4	8.48	4.25	1.64, 1.72	1.31, 1.36	1.64	εH 2.94	7.0
Leu 5	8.43	4.29	1.56	1.56	0.95		8.0
Ile 6	8.57	4.15	1.83	1.16, 1.50	0.87	γCH_3 0.87	9.7
Leu 7	8.62	4.43	1.55	1.65	0.86, 0.92		8.0
Asn 8	8.71	4.71	2.80, 2.84			NH_2 7.08, 7.70	8.7
Gly 9	8.56	3.92, 3.99					6.7
Lys 10	8.35	4.41	1.77, 1.85	1.41, 1.46	1.68	εH 2.99	6.7
Thr 11	8.39	4.34	4.18	1.23			7.7
Leu 12	8.51	4.39	1.57, 1.63	1.63	0.83, 0.93		8.0
Lys 13	8.60	4.29	1.77, 1.83	1.43, 1.46	1.68	εH 2.99	8.7
Gly 14	8.60	3.98, 3.98					7.7
Glu 15	8.37	4.49	2.02, 2.15	2.49			5.7
Thr 16	8.51	4.48	4.27	1.24			7.7
Thr 17	8.44	4.49	4.28	1.23			7.3
Thr 18	8.38	4.38	4.25	1.23			6.7
Glu 19	8.51	4.40	2.21	2.48			7.7

mentally determined to be also very small (Jiménez et al., 1987, 1992). Figure 5b shows the Hα δ differences between H_2O and TFE/H_2O represented against the amino acid sequence of the 2–19 fragment.

Size Exclusion Chromatography. In TFE/H_2O the 2–19 fragment of B_1 domain elutes at a volume corresponding to a molecular mass of 1953 daltons, very close to that of the monomer, 2011 daltons. Similar results were obtained in pure H_2O. They indicate that aggregated species, if any, are not significantly populated under the conditions used in the present NMR study.

Secondary Structure Predictions. The probabilities of formation of all possible four-residue β-turns in the 2–19 peptide chain, as evaluated by the method of Chou and Fasman (1977), are shown in Figure 6. No secondary structure prediction was obtained for sequence corresponding to the 2–19 fragment of protein-G using the program Fugue (Rooman et al., 1992). This means that there was not a sizeable energy gap between the computed set of lowest energy structures and the next, different, set closest in energy (Rooman et al., 1992). The backbone conformation predicted for the 2–19 fragment using the program Prelude (Rooman et al., 1991) is shown in Table 2. It can be seen that residues 2–7 prefer helical states, residues 8–9 and 14–15 prefer turn-like states, and the remaining ones prefer extended conformations. Therefore both methods agree in predicting turns in the regions 8–9 and 14–15 of the 2–19 peptide chain, although with small predictive power.

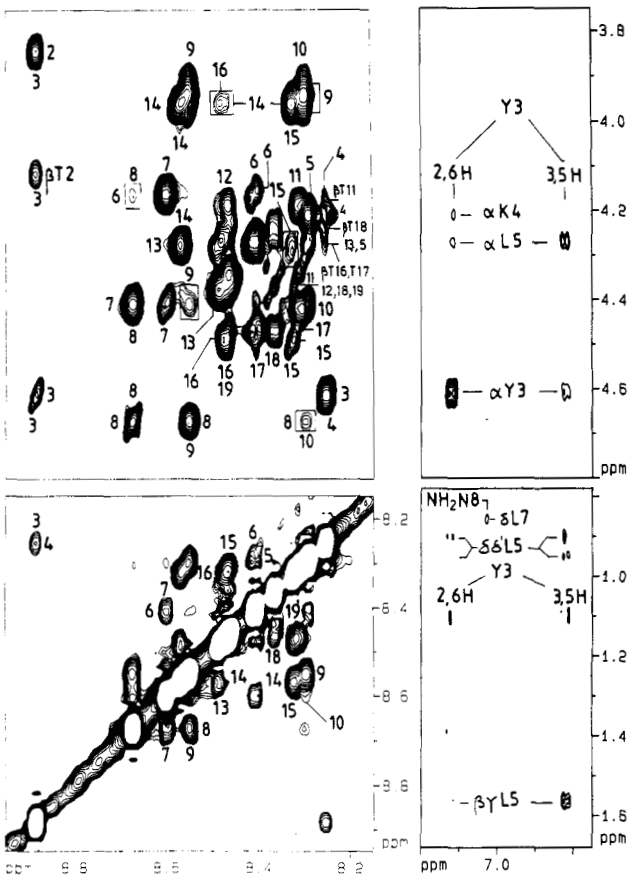

FIGURE 3: Selected regions of the NOESY spectrum of the 2–19 fragment recorded in 9:1 H_2O/D_2O, pH 3.0, at 5 °C, with a 150-ms mixing time. Nonsequential NOEs are shown boxed.

Three-Dimensional Structures. It is well known that a rigorous interpretation of short peptide NOE intensities in geometric structural terms is not possible due to the problem of multiple structures (conformational flexibility) and the absence of an unique correlation time for the molecule (segmental mobility). However, in cases where an appreciable population of the secondary structure exists, it is not uncommon (Ni et al., 1992; Sönnichsen et al., 1992; Kemmink et al., 1993) to look for 3D model structure(s) compatible with the experimental NOEs. This type of calculation was performed for the 2–19 fragment using the NOE data set obtained in TFE/H_2O solution and distance geometry procedures (Güntert et al., 1991), the resulting structures being shown in Figure 7. If used with caution, because by no means do they represent the only conformations adopted by the peptide chain, they are very useful because they give a visualization of what the NOE compatible conformers must look like.

DISCUSSION

Structure of the 2–19 Fragment in Aqueous Solution. The CD spectrum of the 2–19 fragment in H_2O (Figure 2) is compatible with a flexible peptide without signs of a significantly populated folded structure. These results should not be interpreted as a definitive absence of conformational preferences because local, low populated, folding in peptides may be not detected by CD (Dyson et al., 1990). One typical example is the so called "nascent" helix (Dyson et al., 1988b). The addition of urea causes a small, but detectable, shift toward more positive ellipticity values, consistent with the presence of more disordered states in that condition.

The NOE data provide a more discriminating view of the possible folded states of the 2–19 fragment in aqueous solution.

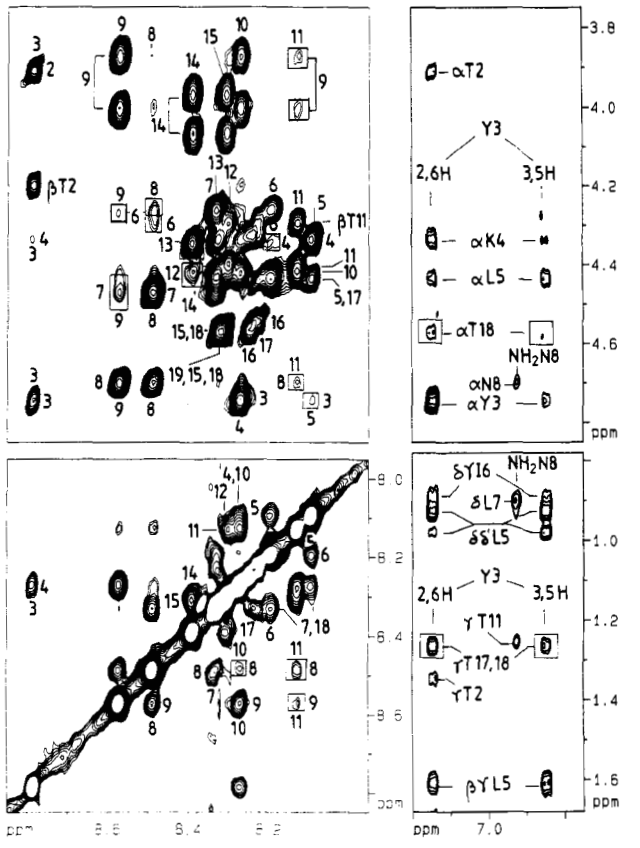

FIGURE 4: Selected region of the NOESY spectrum of the 2–19 fragment recorded in 30% TFE/H_2O, pH 3.0, at 5 °C, with a 150-ms mixing time. Nonsequential NOEs are shown boxed.

The NOE summary (Figure 5a) shows that, in addition to $\alpha N(i,i+1)$ sequential NOEs typical of extended peptide chains, a set of sequential NN NOEs was also detected. Their intensities, when compared with those of their corresponding $\alpha N(i,i+1)$ NOEs, were small ($I_{NN}/I_{\alpha N} < 0.15$), indicating that the possible folded states have small populations. The variation of the relative intensities of NN NOEs along the chain seems to indicate that there are two regions of the peptide chain that show some deviation from fully randomized ϕ,ψ angles; they span from residues 7–10 and 13–16 (Figure 5a). In these two regions the $NN(i,i+1)$ NOEs show intensity maxima that are accompanied by parallel maxima in the intensities of the $\alpha N(i,i)$ NOEs and minima in the intensities of the $\alpha N(i,i+1)$ NOEs. Interestingly, it is also in these two regions of the peptide chain where $\alpha N(i,i+2)$ NOEs appear, which confirms the presence of local folded structures. At the N- and C-terminal residues, the absolute intensities of all NOEs decrease (Figure 5a). This is expected from the shorter local correlation times in those regions of the peptide chain, and it has been observed in other linear peptides (Nieto et al., 1988). Medium-range NOEs of the type $\alpha N(i,i+2)$ are normally interpreted as arising from β-turns (Wüthrich et al., 1984; Reed et al., 1988; Blanco et al., 1991; Dyson et al., 1988a) or nascent helical turns (Dyson et al., 1988b). In the absence of $\alpha N(i,i+3)$ and $\alpha N(i,i+4)$ NOEs, the β-turn interpretation is preferred. It can be seen that the Hα δ shifts upon urea addition are downfield (Figure 5a), thus being interpretable as helix or turn formation in H_2O, and very small if compared with the Hα shift expected for full helix formation, –0.30 ppm (Williamson, 1990) or –0.39 ppm (Wishart et al., 1991), i.e., the populations involved must be very small.

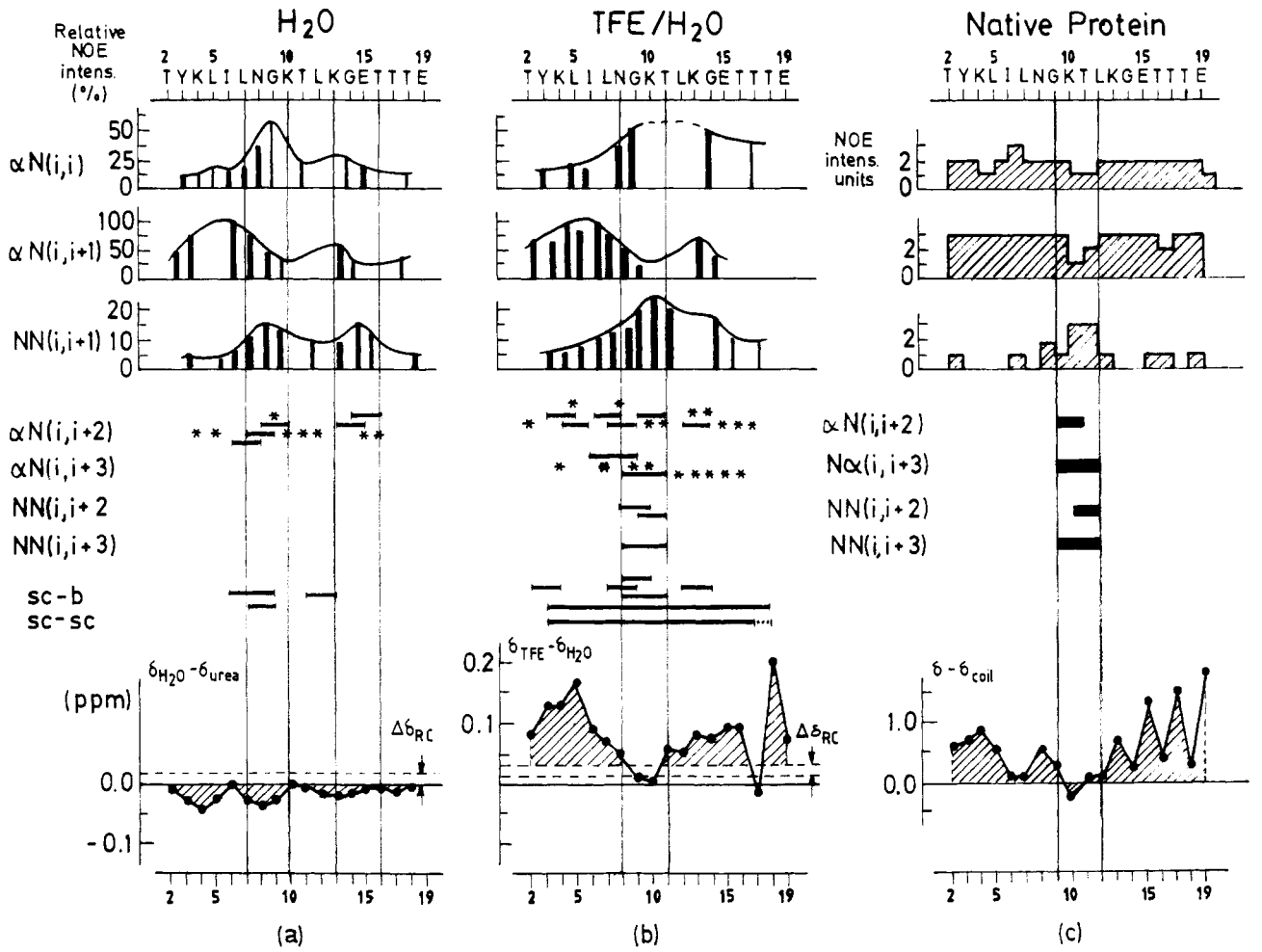

FIGURE 5: (a) Summary of the NOE information obtained for the 2–19 fragment in H_2O solution, at 5 °C, pH 3.0. Intensities corresponding to nonoverlapping NOE cross peaks are represented by thick lines, while those shown by thin lines correspond to partially overlapping ones (see Experimental Procedures). Stars mark NOEs that would not be observable due to resonance overlap. Conformational shifts of the Hα resonances evaluated as $\delta_{H_2O} - \delta_{urea}$ are also shown. For glycine residues the average δ value of the two Hα protons has been represented (b) the same as in panel a but in 30% TFE/H_2O; the Hα conformational shifts were evaluated as $\delta_{TFE} - \delta_{H_2O}$. (c) Pattern of short-range NOEs and Hα conformational shifts of the 2–19 chain region of protein-G B_1 domain evaluated as $\delta - \delta_{coil}$ (Bundi & Wüthrich, 1979) using the reported NMR assignment (Protein Data Bank entry 1GB1.mr). The range of variation of Hα δ values of random tetrapeptides upon 30% TFE (Jiménez et al., 1992) or urea addition ($\Delta\delta_{RC}$) is also shown (Jiménez et al., 1992, 1994).

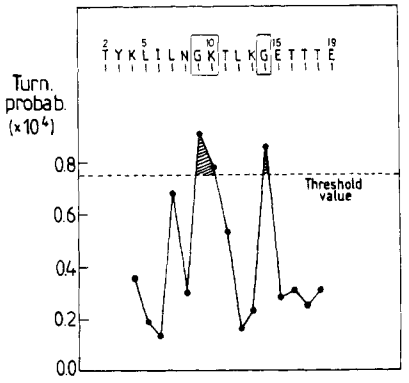

FIGURE 6: Four-residue β-turn prediction calculated for the 2–19 fragment of protein-G B_1 domain using the method of Chou and Fasman (1977). The value shown above that particular residue was the third one of the β-turn. Shaded regions show probability values above the usually quoted threshold value of 0.75×10^4.

Amide solvent accessibility evaluated as amide shift temperature coefficients (Table 1) indicates that none of the amide proton were solvent protected, with the only possible exception of Lys 4, the temperature coefficient of which (−5.0 ppb/K) was just outside the lower limit of the range expected for random peptides (Jiménez et al., 1986). It should be noted that Lys 4 is adjacent to Tyr and the presence of an aromatic residue in a peptide chain may give rise to anomalous low amide shift temperature coefficients of nearby residues, arising from changes in rotomer populations of the aromatic side chain, as recently reported for N-terminal peptides of bovine pancreatic trypsin inhibitor (Kemmink et al., 1993). The partial "solvent protection" of the amide proton of Lys 4 is, however, lost upon urea addition, as evidenced by the large increase of the corresponding amide shift temperature coefficient (Table 1).

It is interesting to compare the experimentally detected folding of the 2–19 fragment with secondary structure predictions. The turn probability, computed by the method of Chou and Fasman (1977), is above the accepted threshold value in the peptide regions where the two Gly residues are located (Figure 6), the same regions where, according to NMR, turn formation is detected. The region spanning residues 2–7 is predicted to be helical by the method of Rooman et al. (1991) (Table 2), but the weak NN NOEs detected and the absence of medium-range NOEs in that region indicate to the contrary. However, the small Hα downfield shifts detected upon urea addition around Lys 4, outside the "random coil" range, are compatible with a very small helical turn population in that chain region (Figure 5a). Residues 10–13 and 16–18

Table 2. Predicted Conformational States for the Residues of the 2–19 Fragment of Protein-G β_1 Domain Computed According to the Method of Rooman et al. (1991)

conformation number	rms differences between states (Å)	conformational state[a] 2 T	3 Y	4 K	5 L	6 I	7 L	8 N	9 G	10 K	11 T	12 L	13 K	14 G	15 E	16 T	17 T	18 T	19 E	computed energy (kcal/mol)
1		A	A	A	A	B	A	C	G	B	B	B	B	B	B	P	B	B	X	−2.99
2	2.80													E						−2.96
3	3.62					A														−2.94
4	3.56														C					−2.92
5	4.48					A								E						−2.91
6	6.12													E	C					−2.89
7	1.72														P					−2.88
8	1.34													P						−2.88
9	5.62					A									C					−2.87
10	4.45													E	P					−2.86
11	7.49					A								E	C					−2.84
12	0.85															B				−2.84
13	4.43					A									P					−2.83
14	3.29					A								P						−2.82
15	0.63																P			−2.82
16	3.36				B															−2.82
17	2.98													P	C					−2.81
18	3.27													E		B				−2.81
19	2.35			B																−2.81
20	6.05					A								E	P					−2.80

[a] A, α-helix; B, β-strand; C, 3_{10}-helix; E, extended; G, left-handed helix; P, extended; X, not computed; ψ and ϕ torsional angles corresponding to these conformational states are defined in Rooman et al. (1991). For clarity only the states that differ from conformation no. 1 (the lowest energy conformation) are shown.

FIGURE 7: Stereoview of the four three-dimensional structures of the 2–19 fragment, that are compatible with the experimental NOE restrictions detected in TFE/H_2O solution. They were modeled using the DIANA program (Güntert et al., 1991). The N1–N4 labels show the N-terminal ends of the peptide chains.

are predicted to be extended, in essential agreement with NOE and chemical shift data.

In summary, the structure of the 2–19 fragment seems to be basically a flexible one in H_2O solution, with two low populated turn-like structures (β-turn or nascent helix) at residues 8–9 and 14–15 and possibly helical also at residues 3–5, in close agreement with the secondary structure predictions. It should be mentioned that none of these features are coincident with the native β-turn in the protein, which occurs at residues 9–12 (Figure 1). There are no NMR signs of formation of the native antiparallel β-sheet (Figure 1), i.e., no cross-sheet NOEs are detected and downfield Hα shifts are observed upon urea addition, the opposite sense expected if partial β-sheet formation was present in the absence of urea. It seems that the large stability of the B_1 domain does not originate from a strong secondary structure preference for its isolated peptide segments, at least of the N-terminal β-hairpin investigated here.

Structure of the 2–19 Fragment in TFE/H_2O Solution. A first indication that the addition of TFE originates a conformational change in the peptide is the ellipticity changes around 195 and 217 nm observed in the CD spectrum as compared with values in H_2O (Figure 2). The CD spectrum in TFE/H_2O solution does not show the double minimum at 208 and 222 nm typical of helices (Johnson, 1988), but it rather resembles the one expected for a mixture of coil and variable proportions of sheet and/or turn. Qualitatively, the CD trace showing the difference between TFE/H_2O and H_2O resembles the typical β-sheet CD curve (Figure 2). The average percentages of secondary structure obtained from the CD curve in TFE/H_2O using three different decomposition methods (see Experimental Procedures) were 23% random, 4% helix, 36% turn, and 37% sheet. Although the use of protein CD reference spectra to decompose a peptide CD curve will provide results of limited accuracy, they are sufficient to stablish on the one hand that negligible amounts of helix are being formed in TFE/H_2O by the protein G 2–19 fragment. They show, on the other hand, that sheet and/or turn conformations in addition to coil states are needed to explain the experimental CD spectrum. These CD results reinforce the notion that TFE induced conformational changes in peptides are not due to a general helix-promoting property of this solvent, independent of the peptide amino acid sequences involved.

The variation along the peptide chain of the sequential NN and αN NOE intensities observed in the 2–19 fragment is remarkably different in TFE/H_2O and in pure H_2O (Figure 5). The largest NN(i,i+1) NOEs observed in TFE/H_2O solution are now those connecting residues 9–10, 10–11, and 11–12, which are accompanied by a minimum in the intensities

of the corresponding $\alpha N(i,i+1)$ NOEs. The increase of the $NN(i,i+1)$ NOE intensities also indicates an increase of the population of chain conformers having dihedral ψ,ϕ angles in the α region of the conformational map, i.e., turn-like or helix-like. A more dense pattern of medium-range NOEs appear also in the same chain region, residues 8–11, thus confirming that the conformational change was affecting those residues (Figure 5b).

It is interesting to compare the NOEs detected for the isolated 2–19 fragment with the NOEs actually observed for the same amino acid residues in the intact domain (Figure 5c). It may be seen that relative intensities of NN and αN NOEs and the presence of several medium-range $(i,i+2)$ and $(i,i+3)$ NOEs at the β-turn are similar in the protein and the fragment, which suggests the conformational features of the peptide chain in the region 8–11 are also similar in the two states. Particularly important is the presence of two long-range NOEs in the NOESY spectrum of the 2–19 fragment in aqueous trifluoroethanol (Figure 4). One is connecting side chain protons of Tyr 3 to the Hα proton of Thr 18, and the other one connects the same Tyr 3 side chain protons to methyl groups of either Thr 17 or Thr 18. These NOE cross peaks can be explained, once aggregation is discarded, only by the existence of hairpin-like folded structures, which in turn necessarily implies a reversing turn of the peptide chain. The presence of a turn involving residues 8–11 is additionally supported by the amide solvent protection data in TFE/H_2O solution. The shift temperature coefficient of Thr 11 is significantly smaller in TFE/H_2O (–5.1 ppb/K) than in H_2O solution, just outside the lower limit measured for "random coil" peptides (Jiménez et al., 1986), while all the remaining amide protons of the peptide chain are within the normal range (Table 1). This is the situation expected if Thr 11 were the fourth residue of a regular type I β-turn involving residues 8–11 in which the typical (Rose et al., 1985) $i+3 \rightarrow i$ hydrogen bond were present. Under denaturing conditions (6 M urea) the temperature coefficient of Thr 11 amide proton became normal, i.e., exposed to solvent (–7.7 ppb/K).

The Hα proton chemical shifts give additional information useful for characterizing the low populated folded structure adopted by this 2–19 fragment. Downfield Hα shifts upon TFE addition were detected for residues 2–8 and 11–19 (except Thr 17), which indicates an increase in the population of local conformers with ϕ,ψ angles corresponding to highly extended peptide chains. This result agrees with the existence of β-sheet conformations deduced from the analysis of the CD spectrum and with the presence of the cross-sheet long-range NOEs already mentioned. In contrast, Hα signals of residues 9 and 10 do not shift or shift in the opposite sense (upfield) upon TFE addition, consistent with β or helical turn formation in those residues, in agreement with the relatively intense NN NOEs detected for the same two residues. The TFE induced shifts on the Hα signals of the isolated 2–19 fragment of the B_1 domain and the Hα conformational shifts of the same residues in the native B_1 domain are qualitatively similar, in both the sheet and turn regions (Figure 5c), lending additional support to the hypothesis that TFE stabilizes a 2–19 peptide chain conformation similar to the one in the native protein.

In summary, the agreement among CD, NOE, amide solvent protection, and chemical shift data leads us to conclude that the 2–19 fragment adopts in TFE/H_2O solution a set of β-hairpin-like structures very similar to the native one, i.e., having the β-turn located at nearly the same point of the peptide chain. This set of β-hairpins are in exchange with more extended conformations. It is evident that β-hairpin-like structures will of neccessity result when long-range cross-strand NOEs are included in the constraints used in structure calculations. As shown in Figure 7, the N- and C-terminal peptide ends are in proximity and basically in an extended conformation in all the computed NOE compatible structures, while in the central region of the peptide chain turn-like structures predominate in agreement with the independent CD and chemical shift data. Thus, the global fold corresponds basically to a hairpin-like structure, although the two β strands may be flexible and not highly packed as in a native protein, i.e., the structure is somewhat reminiscent of a molten-globule state. The β-hairpin structures proposed are not "crystal-like", i.e., chain flexibility and low populations are present, features that may explain the absence of $\alpha\alpha$ interstrand NOEs and the lack of solvent protection for β strand amide protons. The only two cross-sheet NOEs detected, involving Tyr 3 and Thr 18 side chains, are very favorable to be detected from the point of view of signal/noise ratio (i.e., side chain resonances are narrow, corresponding to several equivalent protons, and are in a region of the NMR spectrum free of other resonances). The situation is very different for $\alpha\alpha$ interstrand NOEs, because the corresponding NMR signals are one proton intensity multiplets and they lie in a crowded region of the spectrum close to the diagonal peaks. Therefore, it is not very surprising that $\alpha\alpha$ interstrand NOEs, expected for a regular β-hairpin structure, were not detected in the hairpin formed by the 2–19 fragment in TFE/H_2O solution. For larger β-hairpin populations, $\alpha\alpha$ interstrands NOEs became detectable (Blanco et al., 1993). The side chain of Tyr 3 also shows nonsequential NOEs to the methyl groups of Leu 5 and Ile 6 (Figure 4), in agreement with the existence of a molten globule-like state where side chain mobility is possible. Its presence only limits the interpretation of β-hairpin formation by the 2–19 fragment in the sense that a hairpin is not the only structure present in solution, i.e., other conformers exist. On the other hand, they cannot, alone, override other evidence of β-hairpin formation arising from CD, H_α conformational shifts, and the aforementioned Tyr 3–Thr 18 long-range NOEs. The important point is why the polypeptide chain folds back in TFE/H_2O solution to mimic the final native structure, not if side chains adopt other nonnative conformations, most probably due to the low population of the β-hairpin conformers plus side chain flexibility, as already mentioned.

Effect of TFE on the Peptide Structure. We have found that TFE is able to increase the population of a native-like β-hairpin in an isolated fragment of the B_1 domain of protein-G to a detectable level. The immediate question to be answered is, Why in TFE? The way in which the medium surrounding a polypeptide chain affects its structure is still poorly understood, although some reports indicate the medium is as important as the amino acid sequence itself (Barrow & Zagorski, 1991; Zhong & Johnson, 1992; Wu et al., 1993; Thomas & Dill, 1993). For the particular case of TFE, several reasons have been proposed to explain its effects on peptide structure (Nelson & Kallenbach, 1986; Sönnichsen et al., 1992; Buck et al., 1993). It has been argued that the reduced dielectric constant of TFE (as compared with that of pure water) favors intramolecular hydrogen bonds rather than hydrogen bonds to solvent. Another reason is that possible stabilizing interactions between charged groups of the peptide chain are less shielded in TFE than in water, favoring a folded state. In our opinion, one important fact that should be also taken into account is that, experimentally, phospholipid micellar systems stabilize peptide helices in much the same manner as TFE (Briggs & Gierasch, 1984; Macquaire et al.,

1992; Rizo et al., 1993). Moreover, in some cases the increase in helix population is similar when using either alcohols or micelles (Briggs & Gierasch, 1984; Bruch et al., 1989; Strickland et al., 1993). Since a hydrophobic environment in the vicinity of the peptide molecules is common to TFE and micellar media, it is possible that in this environment the folding tendencies coded in particular amino acid sequences are realized to a greater extent. The idea that a hydrophobic environment may stabilize or even induce native-like structures in a peptide chain is supported by other recent experimental results. For example, it has been reported (Macquaire et al., 1993) that an annexin I fragment forms a native-like helix–turn–helix tertiary motif in a micellar system. Lysozyme (Buck et al., 1993), ubiquitin (Stockman et al., 1993), and peptide fragments from α-lactalbumin (Alexandrescu et al., 1993) maintain many native-like structural characteristics in TFE-containing solutions. In addition, native-like turns (not hairpins) have been detected in isolated fragments of actin (Sönnichsen et al., 1992) and myoglobin (Shin et al., 1993) in TFE-containing solutions.

The striking point, because of its relevance in the protein folding problem, is not why a conformational change occurs in the 2–19 fragment upon a solvent change, but rather why the native structure is stabilized in TFE instead of pure H_2O. If unspecific interactions drive the hydrophobic collapse of a nascent protein into a molten-globule-like state (Kuwajiwa, 1989), it should not be too surprising for a hydrophobic environment, such as the one created by alcohol addition, to stabilize secondary structures similar to the final native ones. This does not imply that the alcohol always simulates the protein environment; the effect may be dependent on the nature of the amino acid sequences involved and possibly also on the relative importance of tertiary, native or nonnative, hydrophobic interactions between that particular chain segment and the rest of the protein. In fact, TFE does not always induce native-like structures in protein fragments, the 12–26 fragment of tendamistat, for example, showed native-like β-turn formation in H_2O (Blanco et al., 1991), but a helix was stabilized upon TFE addition (Jiménez et al., 1992). Also it has been noted that extra, nonnative helices are induced by TFE in proteins (Fan et al., 1993; Yang & Mayo, 1993) and peptide fragments(Sönnichsen et al., 1992).

The effect of alcohols in switching protein structure has been very recently examined from a theoretical point of view (Thomas & Dill, 1993). Despite the limitation of the model, two-dimensional short peptide chains, and only hydrophobicity and helix propensities driving the folding, its predictions are very interesting in connection with the experimental results we found in this work. In Dill's model, it is predicted that the solvent can switch from one unique conformation (H_2O) to another unique conformation (TFE), depending on the amino acid sequences involved. The effect of TFE was modeled by weakening the hydrophobic interactions and enhancing helical interactions, it being the balance between the two (sequence dependent) which controls the actual conformation adopted by the peptide chain. This simple model offers an explanation, alternative to the one suggested above, for the experimental fact that TFE stabilizes peptide helices or sheets in a sequence-dependent manner.

Protein Folding Implications. The idea that short segments of protein chains in general (Rose et al., 1976; Kim & Baldwin, 1982) and β-turns in particular (Lewis et al., 1971; Kuntz, 1972; Wright et al., 1988) may play an active role in protein folding processes has been suggested on several occasions. Recent studies with isolated protein fragments show that native β-turns may have sufficient stability to be detected by NMR (Blanco et al., 1991; Sönnichsen et al., 1992; Shin et al., 1993). We have reported in this paper the detection, in the isolated N-terminal fragment of the protein-G B_1 domain, of a β-hairpin structure that is essentially that observed in the final native structure of the protein. This suggests that not only β-turns but also β-hairpins may play a role in directing protein folding. Our results also suggest that the structural determinants of the folded β-hairpin structure are short-range coded. Although it is certainly possible that long-range interactions may help in stabilizing the hairpin formed in this protein, they do not appear to define its extent. Local encoding of a β-hairpin may have an important effect in the protein folding process, by directing the search of the conformational space. In fact, theoretical simulations of folding have shown that small populations of native-like preferred conformers are sufficient to drive plastocianin to its correct native fold (Skolnick & Kolinski, 1990).

The role of turns in folding has also been investigated using engineered proteins. It has been shown (Hynes et al., 1989) that one turn can be transferred from concanavalin to staphylococcal nuclease while maintaining the turn geometry of concanavalin as well as the structure and the biological activity of the nuclease. This result indicates that very few amino acid residues are needed to define the turn geometry and that this geometry is barely affected by nearby protein residues, in agreement with the results reported here. It should be mentioned that random mutations of a three-residue turn in cytochrome b_{562} did not affect the folding or activity of the protein (Brunet et al., 1993). However, in our opinion this result does not necessarily imply that turns are not important in early stages of folding; rather, it reinforces the idea that proteins are generally very tolerant to minor changes in sequence (Rennell et al., 1991). Since there are many possible contributions to the stability of a folded protein, substitution experiments that modify a few residues are more difficult to interpret in proteins than in isolated protein fragments, where no long-range interactions are present.

Finally, it should be noted that the complete protein-G B_1 domain folds into the native state in aqueous solution, but its isolated N-terminal fragment needs a less polar aqueous trifluoroethanol medium to produce detectable levels of native conformational preferences. The environment surrounding one particular chain segment in a partial folded state of a protein need not be necessarily polar. In fact, relatively apolar solvents, such as alcohols, are thought (Ponnuswamy, 1993) to better represent the interior of a protein. It is possible that the aqueous trifluoroethanol medium simulates, better than pure water, the protein environment in which the 2–19 fragment folds when forming part of the complete B_1 domain.

Conclusions. The work reported here is, to our knowledge, the first example of the stabilization by TFE of a basically monomeric native-like β-hairpin structure in an isolated protein fragment, the structure being supported by the presence of long- and medium-range NOEs and proton conformational shifts. Although the mechanism by which the stabilization is achieved is not well understood, it is striking that the native-like structure was detected in TFE, because, in principle, native structures in proteins are more stable in water. What is important is that the 2–19 peptide chain has a tendency to

[2] One such study became available during the review process (Cox et al., 1993), where methanol-driven native β-hairpin formation was detected by NMR in the N-terminal fragment of ubiquitin, results that fully agree with ours and reinforce the hypothesis of a role for β-hairpin in protein folding.

fold at a point very close to the final native β-turn locus and that this folding is sufficient to induce sheet formation detectable by NMR under appropriate conditions, which supports the idea that β-hairpin formation may play an active role in protein folding processes. The study of the conformation of protein fragments continues to be a valid approach to investigate early protein folding events. Additional conformational studies[2] of other protein fragments, potential β-hairpin formers, are needed to understand why TFE stabilizes this native-like structure in peptides having particular amino acid sequences.

ACKNOWLEDGMENT

We thank N. H. Andersen for text revision and for helpful comments on the manuscript and S. Wodak and G. Deléage for the computer programs. Excellent technical assistance from C. López, A. Gómez, and L. de la Vega is also acknowledged.

SUPPLEMENTARY MATERIAL AVAILABLE

One ROESY and one NOESY spectra recorded in TFE/H_2O using mixing times of 200 and 80 ms, respectively, plus one 150-ms NOESY spectrum recorded in TFE/H_2O at pH 2.5 (3 pages). Ordering information is given on any current masthead page.

REFERENCES

Alexander, P., Fahnestock, S., Lee, T., Orban, J., & Bryan, P. (1992) *Biochemistry 31*, 3597–3603.
Alexandrescu, A. T., Evans, P. A., Pitkeathly, M., Baum, J., & Dobson, C. M. (1993) *Biochemistry 32*, 1707–1718.
Andersen, N. H., Cao, B., & Chen, C. (1992) *Biochem. Biophys. Res. Commun. 184*, 1008–1014.
Bansai, A., & Gierasch, L. M. (1991) *Cell 67*, 1195–1201.
Barrow, C., & Zagorski, M. G. (1991) *Science 153*, 179–182.
Bax, A., & Davies, D. G. (1985) *J. Magn. Reson. 65*, 355–360.
Bierzynski, A., Kim, P. S., & Baldwin, R. L. (1982) *Proc. Natl. Acad. Sci. U.S.A. 79*, 2470–2474.
Blanco, F. J., Jiménez, M. A., Rico, M., Santoro, J., Herranz, J., & Nieto, J. L. (1991) *Eur. J. Biochem. 200*, 345–351.
Blanco, F. J., Jiménez, M. A., Rico, M., Santoro, J., Herranz, J., & Nieto, J. L. (1992a) *Biochem. Biophys. Res. Commun. 182*, 1491–1498.
Blanco, F. J., Herranz, J., González, C., Jiménez, M. A., Rico, M., Santoro, J., & Nieto, J. L. (1992b) *J. Am. Chem. Soc. 114*, 9676–9677.
Blanco, F. J., Jiménez, M. A., Rico, M., Santoro, J., & Nieto, J. L. (1993) *J. Am. Chem. Soc. 115*, 5887–5888.
Bolotina, I. A., Checkov, V. O., Lugauskas, V. Yu., & Ptitsyn, O. B. (1980) *Mol. Biol. 14*, 709–715.
Braun, W., Wider, G., Lee, K. H., & Wüthrich, K. (1983) *J. Mol. Biol. 169*, 921–948.
Briggs, M. S., & Gierasch, L. M. (1984) *Biochemistry 23*, 3111–3114.
Bruch, M. D., McKnight, C. J., & Gierasch, L. M. (1989) *Biochemistry 28*, 8554–8561.
Bruix, M., Perelló, M., Herranz, J., Rico, M., & Nieto, J. L. (1990) *Biochem. Biophys. Res. Commun. 167*, 1009–1014.
Brunet, A. P., Huang, E. S., Huffine, M. E., Loeb, J. E., Weltman, R. J., & Hecht, M. H. (1993) *Nature 364*, 355–358.
Buck, M., Radford, S. E., & Dobson, C. M. (1993) *Biochemistry 32*, 669–678.
Bundi, A., & Wüthrich, K. (1979) *Biopolymers 18*, 285–297.
Chandrasekhar, K., Profy, A. T., & Dyson, H. J. (1991) *Biochemistry 30*, 9187–9194.
Chang, C. T., Wu, C.-S., Yang, J. T. (1978) *Anal. Biochem. 91*, 13–31.
Chou, P. Y., & Fasman, G. D. (1977) *J. Mol. Biol. 115*, 135–175.
Cox et al. (1993) *J. Mol. Biol. 234*, 483–492.
Deléage, G., & Geourjon, C. (1993) *Comput. Appl. Biosci. 9*, 197–199.
Dyson, H. J., & Wright, P. E. (1991) *Annu. Rev. Biophys. Biophys. Chem. 20*, 519–538.
Dyson, H. J., Cross, K. J., Houghteen, R. A., Wilson, I. A., Wright, P. E., & Lerner, R. A. (1985) *Nature 318*, 480–483.
Dyson, H. J., Rance, M., Houghteen, R. A., Lerner, R. A., & Wright, P. E. (1988a) *J. Mol. Biol. 201*, 161–200.
Dyson, H. J., Rance, M., Houghteen, R. A., Wright, P. E., & Lerner, R. A. (1988b) *J. Mol. Biol. 201*, 201–217.
Dyson, H. J., Satterthwait, A. C., Lerner, R. A., & Wright, P. E. (1990) *Biochemistry 29*, 7828–7837.
Dyson, H. J., Merutka, G., Waltho, J. P., Lerner, R. A., & Wright, P. E. (1992) *J. Mol. Biol. 226*, 795–817.
Fan, P., Bracken, C., & Baum, J. (1993) *Biochemistry 32*, 1573–1582.
Gill, S. C., & von Hippel, P. H. (1989) *Anal. Biochem. 182*, 319–326.
Gronenborn, A. M., Filpula, D. R., Essig, N. Z., Achari, A., Whitlow, M., Wingfield, P. T., & Clore, G. M. (1991) *Science 253*, 657–661.
Güntert, P., & Wüthrich, K. (1991) *J. Biomol. NMR 1*, 447–456.
Güntert, P., Braun, W., & Wüthrich, K. (1991) *J. Mol. Biol. 217*, 517–530.
Hynes, T. R., Kautz, R. A., Goodman, M. A., Gill, J. F., & Fox, R. O. (1989) *Nature 339*, 73–76.
Jiménez, M. A., Nieto, J. L., Rico, M., Santoro, J., Herranz, J., & Bermejo, F. J. (1986) *J. Mol. Struct. 143*, 435–438.
Jiménez, M. A., Nieto, J. L., Herranz, J., Rico, M., & Santoro, J. (1987) *FEBS Lett. 221*, 320–324.
Jiménez, M. A., Rico, M., Herranz, J., Santoro, J., & Nieto, J. L. (1988) *Eur. J. Biochem. 175*, 101–109.
Jiménez, M. A., Blanco, F. J., Rico, M., Santoro, J., Herranz, J., & Nieto, J. L. (1992) *Eur. J. Biochem. 207*, 39–49.
Jiménez, M. A., Bruix, M., González, C., Blanco, F. J., Nieto, J. L., Herranz, J., & Rico, M. (1993) *Eur. J. Biochem. 211*, 569–581.
Jiménez, M. A., Carreño, C., Andreu, D., Blanco, F. J., Herranz, J., Rico, M., & Nieto, J. L. (1994) *Biopolymers* (in press).
Johnson, W. C. (1988) *Annu. Rev. Biophys. Biophys. Chem. 17*, 145–166.
Kemmink, J., van Mierlo, C. P. M., Scheek, R. M., & Creighton, T. E. (1993) *J. Mol. Biol. 230*, 312–322.
Kessler, H., Gehrke, M., & Griesinger, C. (1988) *Angew. Chem., Int. Ed. Engl. 27*, 490–536.
Kim, P. S., & Baldwin, R. L. (1982) *Annu. Rev. Biochem. 51*, 459–489.
Kraulis, P. J. (1991) *J. Appl. Crystallogr. 24*, 946–950.
Kuntz, I. D. (1972) *J. Am. Chem. Soc. 94*, 4009–4012.
Kuwajima, K. (1989) *Proteins 6*, 87–103.
Lehrman, S. R., Tuls, J. L., & Lund, M. (1990) *Biochemistry 29*, 5590–5596.
Lewis, P. N., Momany, F. A., & Scheraga, H. A. (1971) *Proc. Natl. Acad. Sci. U.S.A. 68*, 2293–2297.
Lian, L.-Y., Yang, J. C., Derrick, J. P., Sutcliffe, M. J., Roberts, G. C. K., Murphy, J. P., Goward, C. R., & Atkinson, T. (1991) *Biochemistry 30*, 5335–5340.
Macquaire, F., Baleux, F., Giaccobi, E., Huynh-Dinh, T., Neuman, J.-M., & Sanson, A. (1992) *Biochemistry 31*, 2576–2582.
Macquaire, F., Baleux, F., Huynh-Dinh, T., Rouge, D., Neuman, J. M., & Sanson, A. (1993) *Biochemistry 32*, 7244–7254.
Nelson, J. W., & Kallenbach, N. R. (1986) *Proteins 1*, 211–217.
Nelson, J. W., & Kallenbach, N. R. (1989) *Biochemistry 28*, 5256–5261.
Ni, F., Ripoll, D. R., & Purissima, E. O. (1992) *Biochemistry 31*, 2545–2554.

Nieto, J. L., Jiménez, M. A., Rico, M., Santoro, J., & Herranz, J. (1988) *FEBS Lett. 239*, 83–87.
Orban, J., Alexander, P., & Bryan, P. (1992) *Biochemistry 31*, 3604–3611.
Peña, M. C., Rico, M., Jiménez, M. A., Herranz, J., Santoro, J., & Nieto, J. L. (1989) *Biochim. Biophys. Acta 957*, 380–389.
Ponnuswamy, P. K. (1993) *Prog. Biophys. Mol. Biol. 59*, 57–103.
Reed, J., Hull, W. E., Lieth, C. W., Kubler, D., Subai, S., & Kinzel, V. (1988) *Eur. J. Biochem. 178*, 141–154.
Rennell, D. Bouvier, S. E., Hardy, L. W., & Poteete, A. R. (1991) *J. Mol. Biol. 222*, 67–87.
Rico, M., Nieto, J. L., Santoro, J., Bermejo, F. J., Herranz, J., & Gallego, E. (1983) *FEBS Lett. 162*, 314–319.
Rizo, J., Blanco, F. J., Kobe, B., Bruch, M. D., & Gierasch, L. M. (1993) *Biochemistry 32*, 4881–4894.
Rooman, M. J., Kocher, J.-P. A., & Wodak, S. J. (1991) *J. Mol. Biol. 221*, 961–979.
Rooman, M. J., Kocher, J.-P. A., & Wodak, S. J. (1992) *Biochemistry 31*, 10226–10238.
Rose, G. D., Winters, R. M., & Wetlaufer, D. B. (1976) *FEBS Lett. 63*, 101–116.
Rose, G. D., Gierasch, L. M., & Smith, J. A. (1985) *Adv. Protein Chem. 37*, 1–109.
Segawa, S. I., Fukuno, T., Fujiwara, K., & Noda, Y. (1991) *Biopolymers 31*, 497–509.
Shin, H. C., Merutka, G. Waltho, J. P., Wright, P. E., & Dyson, H. J. (1993) *Biochemistry 32*, 6348–6355.
Skolnick, J., & Kolinski, A. (1990) *Science 250*, 1121–1125.
Sönnichsen, F. D., Van Eyk, J. E., Hodges, R. S., & Sykes, B. D. (1992) *Biochemistry 31*, 8790–8798.
Stockman, B. J., Euvrad, A., & Scahill, T. A. (1993) *J. Biomol. NMR 3*, 285–296.
Strickland, L. A., Bozzato, R. P., & Kronis, K. A. (1993) *Biochemistry 32*, 6050–6057.
Thomas, P. D., & Dill, K. A. (1993) *Protein Sci. 2*, 2050–2065.
Williamson, M. P. (1990) *Biopolymers 29*, 1423–1431.
Williamson, M. P., Hall, M. J., & Handa, B. K. (1986) *Eur. J. Biochem. 158*, 527–536.
Wishart, D. S., Sykes, B. D., & Richards, F. M. (1991) *J. Mol. Biol. 222*, 311–333.
Wright, P. E., Dyson, H. J., & Lerner, R. A. (1988) *Biochemistry 20*, 7167–7175.
Wu, H., Fan, Y., Sheng, J., & Sui, S.-F. (1993) *Eur. Biophys. J. 22*, 201–205.
Wüthrich, K., Billeter, M., & Braun, J. (1984) *J. Mol. Biol. 180*, 715–740.
Yang, J. T., Wu, C.-S. C., & Martínez, H. M. (1986) *Methods Enzymol. 130*, 208–269.
Yang, Y., & Mayo, K. H. (1993) *Biochemistry 32*, 8661–8671.
Zhong, L., & Johnson, W. C. (1992) *Proc. Natl. Acad. Sci. U.S.A. 89*, 4462–4465.